

High electron temperature associated with the prereversal enhancement in the equatorial ionosphere

K.-I. Oyama,¹ M. A. Abdu,² N. Balan,^{1,3} G. J. Bailey,⁴ S. Watanabe,⁵
T. Takahashi,⁵ E. R. de Paula,² I. S. Batista,² F. Isoda,⁶ and H. Oya⁵

Abstract. High electron temperature in the equatorial ionization anomaly region detected first by Kyokko satellite and later observed frequently by Hinotori satellite are found to be closely associated with the ionization crests of the anomaly. This phenomenon, called the equatorial electron temperature anomaly, is found to occur predominantly in the equinoctial months and to become enhanced with the increase in solar activity. It is mainly a nighttime phenomenon and shows maximum temperature enhancement at around 2100 LT. Using a theoretical model, a mechanism for its occurrence is presented. The mechanism is based on the plasma transport in the evening equatorial ionosphere resulting from the sunset electrodynamic processes.

1. Introduction

The Japanese satellite Kyokko, launched in 1978, encountered regions of high electron temperature T_e over the low-latitude ionosphere during several of its eccentric trajectories. In some cases the temperature enhancement, with respect to the expected nighttime background temperature, exceeded 2000 K [Oyama and Schlegel, 1984]. The region of the enhanced electron temperature extended from magnetic latitude -30° to 7° . The temperature enhancement showed maximum values in the 300° – 310° geographic longitude and -30° to -8° geographic latitude region. Further, it may be noted that this electron temperature enhancement occurred in the region where the electron density was also high. About 16 cases of T_e enhancement were observed out of all the Kyokko passes. It was also noted that all these T_e enhancements occurred in March 1978. Although this was a new finding, a detailed investigation could not be carried out due to the difficulty in identifying its mechanism and the availability of only a small number of observations.

In 1981 the Hinotori satellite was placed into a nearly equatorial (with inclination of 31°) circular orbit at an altitude of about 600 km. This satellite also recorded the phenomenon of the T_e enhancement. During its 17 months of operation, Hinotori frequently observed this phenomenon. The observations described in this paper clearly demonstrate the association of the T_e enhancement with the electron density enhancement of the evening-nighttime equatorial ionization anomaly. Using a theoretical model, a mechanism that invokes the role of the

equatorial ionosphere sunset electrodynamic processes is suggested for the observed anomalous T_e enhancement.

2. Morphology of the Hot Region

Figure 1a shows the electron density, and Figure 1b shows the electron temperature measured by Hinotori on pass 3599. The two shaded regions in Figure 1b represent enhancements in T_e of ~ 600 K and ~ 1000 K at magnetic latitudes 8° and -9° , respectively, with respect to the background T_e values (represented by a dashed curve). These regions coincide with the electron density enhancements of the equatorial anomaly (Figure 1a). The latitudinal structure of the equatorial anomaly is characterized by a trough at the magnetic equator with crests on either side. This feature is reflected clearly in the latitudinal variation of T_e . The equatorial electron temperature anomaly (EETA) is thus associated with the equatorial ionization anomaly (EIA). For a detailed description of the EIA, see Hanson and Moffet [1966], Moffet [1979], Walker and Chan [1989], and Balan and Bailey [1995]. The T_e enhancement of 1500 K with respect to the background at 0500 LT is a sunrise associated phenomenon.

2.1. Global Distribution of the Hot Region

The locations of enhanced T_e with respect to the normally expected background were identified in a large number of Hinotori passes in the evening-premidnight local time sector. The locations so identified are marked by triangles on the trajectory segments of the different passes shown in Figure 2. The magnetic equator is shown by a dashed curve. As Figure 2 shows the hot regions are distributed predominantly at magnetic latitudes away and on either side of the magnetic equator, not on it. Though not shown separately, these locations are also the locations of the electron density enhancements of the EIA crests. The reason for the relatively poor data statistics in the longitude region of 130° – 180° is due to the fact that during the time when the satellite was located in this longitude region the satellite tracking center (Kagoshima) was recovering the data stored from other longitudes.

2.2. Seasonal Dependence

The T_e enhancements which exceed 200 K were separated and are plotted in Figure 3a at the latitudes of their occur-

¹Institute of Space and Astronautical Science, Sagami-hara, Japan.

²National Institute for Space Research, Sao Jose dos Campos, Brazil.

³On leave from the Department of Physics, University of Kerala, Trivandrum, India.

⁴Applied Mathematics Section, School of Mathematics, University of Sheffield, Sheffield, England.

⁵Faculty of Science, Tohoku University, Sendai, Japan.

⁶Faculty of Education, Yokohama National University, Yokohama, Japan.

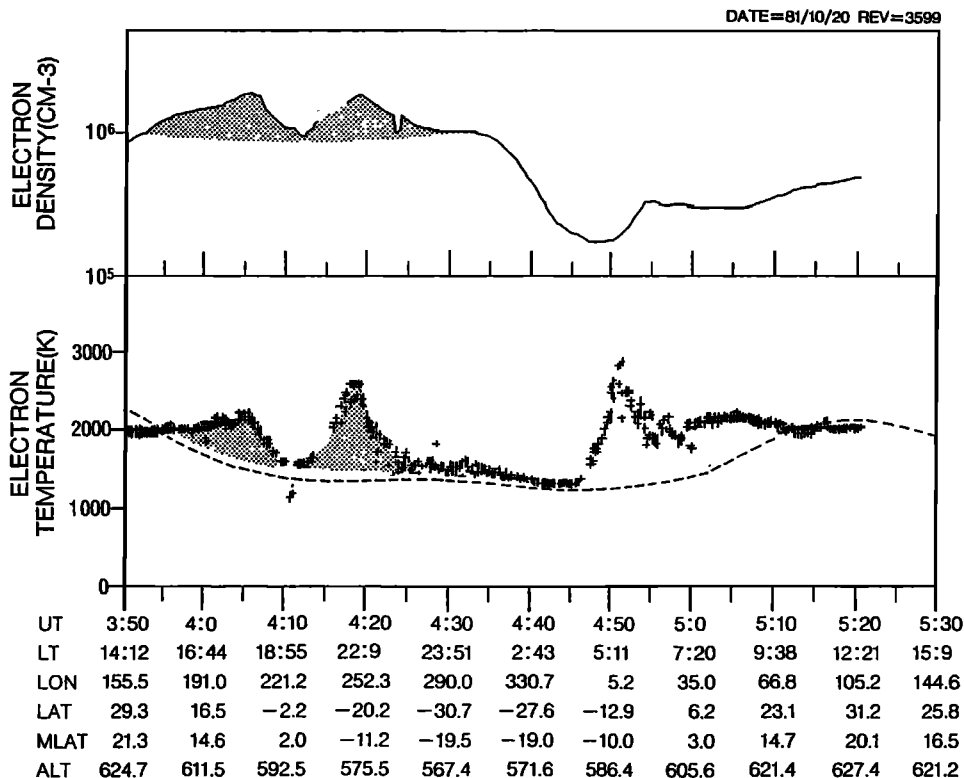


Figure 1. (top) The electron density. (bottom) Electron temperature measured by Hinotori during pass 3599. The two equatorial ionization anomaly (EIA) peaks centered around the magnetic equator at 0410 UT covering the local time interval 1700–2300 LT are associated with the enhanced electron temperatures (shaded regions) with respect to the background temperature and the IRI representation (dashed curve) [Bilitza, 1990]. The T_e enhancement around 0511 LT is the sunrise effect.

rences against the day of the year (top) together with the daily solar flux at 10.7 cm (bottom). The days are counted from January 1, 1981; the Hinotori data started on February 22, 1981, and continued until June 11, 1982. The sizes of the triangles correspond to the degree of departure of the T_e value from its nighttime background value (ΔT_e); the larger the triangle, the larger the T_e enhancement. It is clearly seen that

the larger enhancements are concentrated in the equinoctial months of March and April (around day 90), September and October (around day 270), and again in March and April (around day 450) of the following year. To see the solar activity dependence on the T_e enhancement, ΔT_e was plotted against the solar radio flux at 10.7 cm in Figure 3b. A faint dependence of the T_e enhancement appears to exist in days when the solar

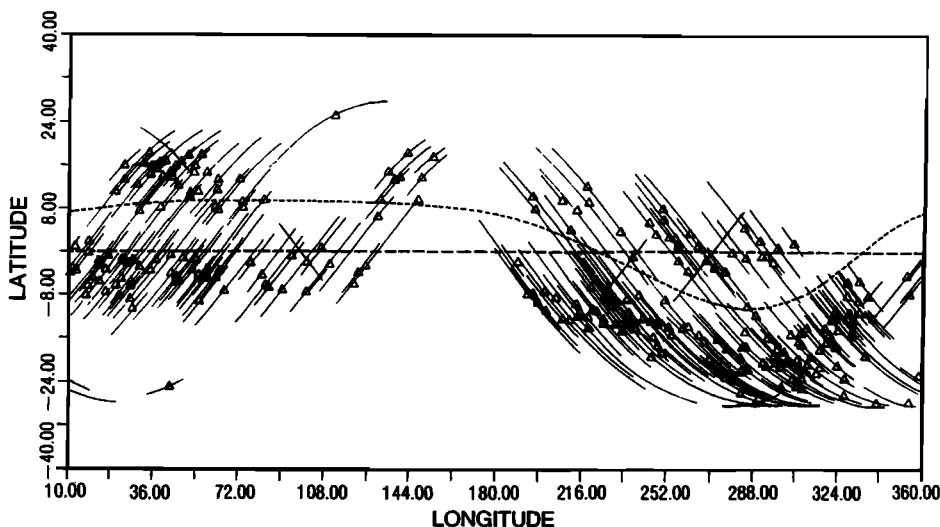


Figure 2. Locations marked in solid lines of enhanced electron temperature along Hinotori trajectory segments, the maximum value of T_e being indicated by triangles. The dashed curve is the magnetic equator.

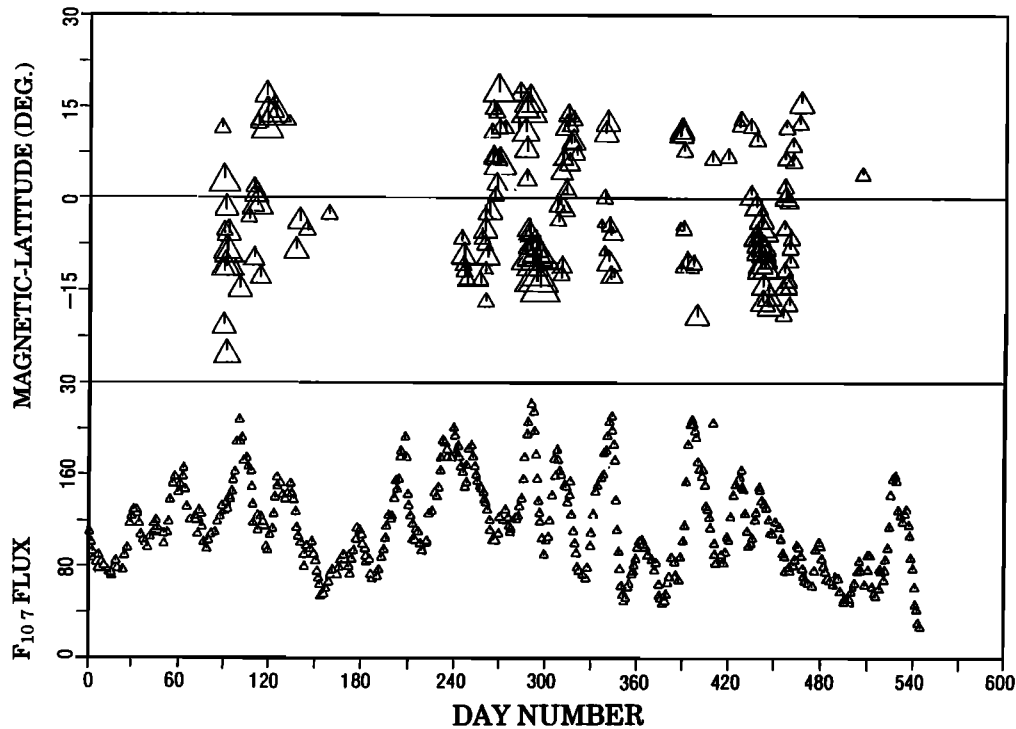


Figure 3a. (top) Occurrence of hot plasma regions marked at geomagnetic latitude versus day number starting from January 1, 1981 (1 month and 20 days before the Hinotori mission), till the end of the Hinotori data on June 11, 1982. Increasing sizes of the plotted triangles indicate increasing T_e deviation (up to 1200 K). (bottom) The solar $F_{10.7\text{ cm}}$ flux diurnal averages for the same period.

flux exceeds about 150 units. In fact, the seasonal distribution of the ΔT_e shown in Figure 3a is somewhat modulated by solar flux values greater than 150 units with ΔT_e generally increasing as the solar flux increases. This modulation is to be specially noted for the cases of increasing flux at around days 345 and 400, which produced enhanced T_e values during December and February, exceptions from the equinoctial occurrence pattern.

2.3. Association With Ground-Based EIA Diagnostics

Cachoeira Paulista (45°W, 22.5°S) in Brazil is situated very close to the EIA crest location. Ionograms obtained from routine soundings over this station were studied when Hinotori flew over Brazil. Although the region surveyed by the ionosonde is not exactly the same as that of the satellite passes, their proximity (in some cases by field line connection) could

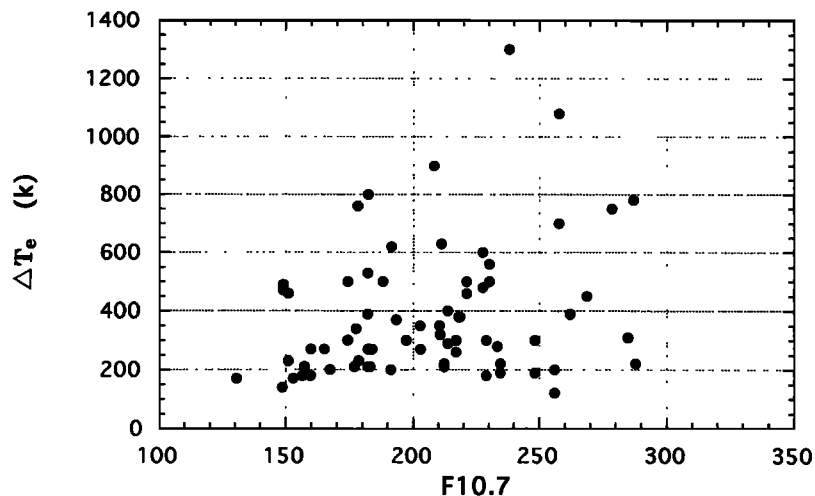


Figure 3b. Departure of T_e from its nighttime background (ΔT_e) versus solar $F_{10.7\text{ cm}}$ flux are plotted in the time period 1900–2100 LT.

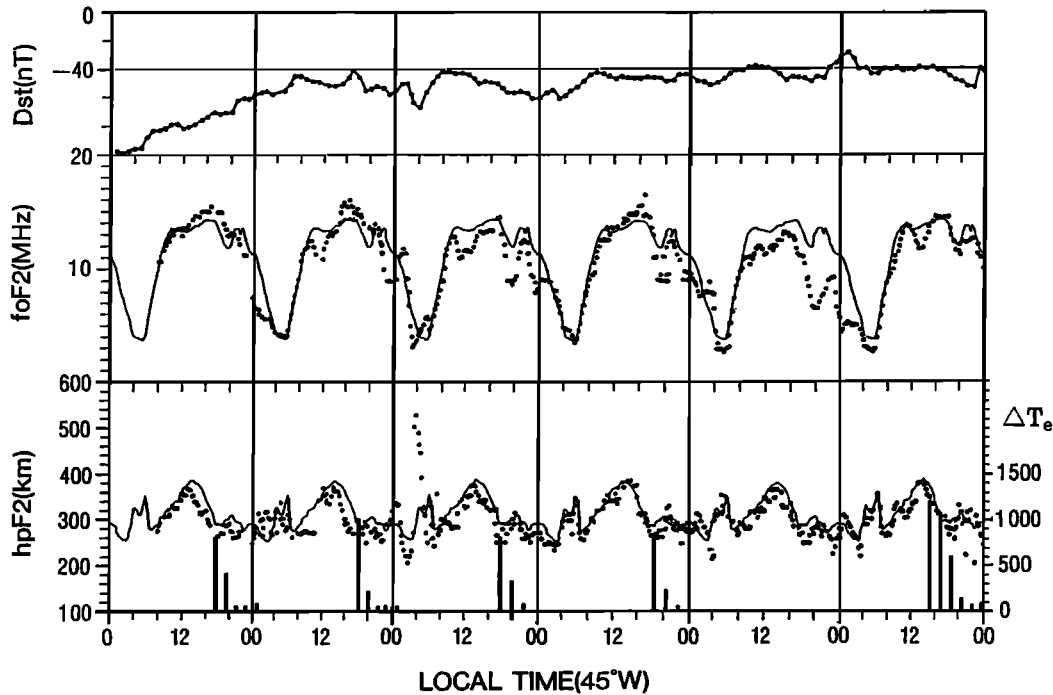


Figure 4. (top) Dst values from May 26 to 31, 1981, for which ionospheric parameters over Cachoeira Paulista ($45^{\circ}W$, $22.5^{\circ}S$) in Brazil are plotted middle panel for f_oF_2 and bottom panel for h_pF_2 (a representative parameter for the F_2 layer peak height). The solid lines represent quiet day mean values, and the dots are values for each day. (bottom) The electron temperature enhancements observed by Hinotori satellite in the vicinity regions of Cachoeira Paulista with scale on the right-hand side.

make a comparison with ionosonde data very valuable in the way of identifying the phenomenon. In Figure 4 are plotted the F layer peak density (critical frequency, f_oF_2) and peak height (h_pF_2) parameters for a few consecutive days of Hinotori passes. The daytime equatorial anomaly produces maximum f_oF_2 values over Cachoeira Paulista at around 1700–1800 LT. Followed by a short-lived decrease in the electron density, there is a resurgence of the EIA starting at approximately 2000 LT. The h_pF_2 values (bottom) that decrease in the afternoon hours show increases again starting at 1800 LT. These increases are produced by the well known prereversal enhancement of the evening equatorial electric field [see, e.g., Woodman, 1970; Fejer et al., 1991]. This electric field enhancement is believed to be produced by the interaction of the eastward blowing thermospheric wind with the Pederson conductivity longitudinal gradient that exists across the sunset terminator [see, e.g., Rishbeth, 1971; Heelis et al., 1974; Farley et al., 1986; Batista et al., 1986]. The electric field enhancement has earlier onset and higher amplitude over the magnetic equator (for example, over Fortaleza, in Brazil than over Cachoeira Paulista [Abdu et al., 1995], where the resulting increase of h_pF_2 is noticeable around 1800 LT. Also marked as vertical bars in the bottom panel of Figure 4 are the T_e enhancements observed during consecutive Hinotori passes over the regions in the vicinity of Cachoeira Paulista. The local times of the temperature enhancements marked in Figure 4 refer to the local times at Cachoeira Paulista ($45^{\circ}W$) when the T_e enhancements were observed by Hinotori. These T_e enhancements have significant longitude-latitude durations so that the local times at Hinotori varied from ~ 1800 LT to ~ 2100 LT. Maximum ΔT_e values observed varied from pass to pass and the peaks occurred reasonably near in time to the onset of the

evening vertical drift enhancements and the formation of the postsunset equatorial anomaly on all these days, which therefore supports the association between the EIA and the EETA. The values of Dst index for these days are also shown in the top panel of Figure 4 to show that ΔT_e increase is not directly related to the geomagnetic disturbance.

2.4. Local Time Variation of EETA

In Figure 5 the maximum value of ΔT_e on each day is plotted against local time from 1800 LT to 0200 LT. There exists a significant scatter in the data. However, a tendency for

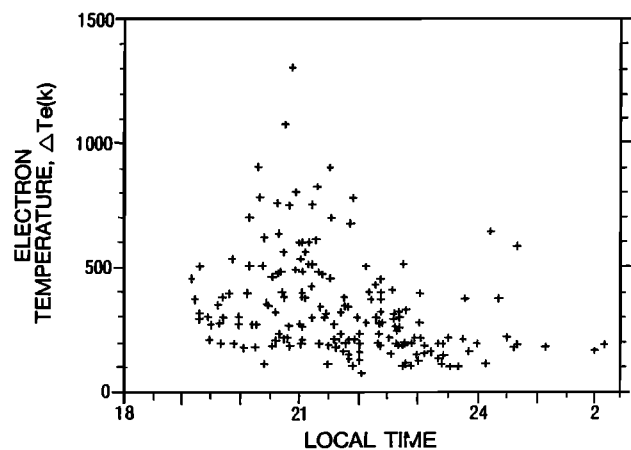


Figure 5. T_e deviation in the center of the hot region (with respect to the background values) plotted as a function of local time during the evening-nighttime period.

ΔT_e to increase from 1800 LT, to reach a maximum value near 2100 LT, and then to decrease to low values by midnight can be noted. The rising part of ΔT_e is due to the continuing influence of the daytime temperature into the nighttime in such a way that the T_e , with respect to an otherwise decaying nighttime (background) temperature, shows up as an increasing function of time. The modified temperature itself starts its decay from 2100 LT onward resulting in the decreasing part of ΔT_e . Maximum T_e of the EETA increases as the associated maximum electron density increases.

3. Mechanism

3.1. Theoretical Modeling

The model values of electron temperature are calculated using the Sheffield University plasmasphere-ionosphere model, SUPIM [Bailey *et al.*, 1993, 1996; Bailey and Balan, 1996]. In this model, coupled time-dependent equations of continuity, momentum, and energy balance are solved along closed magnetic field lines to give values for the concentrations, field-aligned fluxes, and temperatures of the O^+ , H^+ , He^+ , N_2^+ , O_2^+ , and NO^+ ions, and the electrons at a discrete set of points along the field lines. For the present study, the model equations are solved along 112 eccentric-dipole magnetic field lines distributed with apex altitude between 150 and 4000 km; this gives a reasonable 24-hour distribution of model T_e values between 200 and 1500 km altitude and $\pm 30^\circ$ magnetic latitude. The model calculations are for magnetically quiet ($A_p = 4$) equinoctial conditions (day 264) at high solar activity ($F_{10.7} = 238$ and $F_{10.7A} = 210$) and for the longitude of Jicamarca ($77^\circ W$).

The $E \times B$ drift and neutral wind velocities are included in the model calculations. The vertical $E \times B$ drift velocities are obtained from the measurements made at Jicamarca under equinoctial conditions at high solar activity [Fejer *et al.*, 1991]. The drift velocity undergoes a prereversal upward strengthening with peak value of about 45 m s^{-1} at 1845 LT and the velocity reverses downward at about 1930 LT. The Jicamarca drift velocities are used for magnetic field lines with apex altitude less than 450 km. For field lines with apex altitude greater than 3000 km, the drift velocity is taken to be zero. Linear interpolation is used at intermediate apex altitudes. The drift velocity varies along the geomagnetic field lines in accordance with the field line geometry [Bailey and Balan, 1996]. The zonal component of the $E \times B$ drift velocity is neglected since it has only negligible effect on electron density profiles [Anderson, 1981]. The neutral wind velocity in the magnetic meridian, which also varies with altitude and latitude, is determined from the meridional and zonal wind velocities given by the HWM90 thermospheric wind model [Hedin *et al.*, 1991]. The concentrations and temperatures of the neutral gases are taken from the MSIS86 thermospheric model [Hedin, 1987] and the solar EUV fluxes from the EUV94 solar EUV flux model (a revised version of the EUV91 solar EUV flux model [Tobiska, 1991]).

The photoelectron heating rates are calculated by the photoelectron code developed by Richards and coworkers [Richards and Torr, 1988; Torr *et al.*, 1990]. This code, which has been incorporated into SUPIM, uses the two-stream approximation method of Banks and Nagy [1970] and includes interhemispheric transport of photoelectrons. Photoelectrons heat the thermal electrons through Coulomb collisions, magnetic trapping due to pitch angle diffusion, and backscattering from

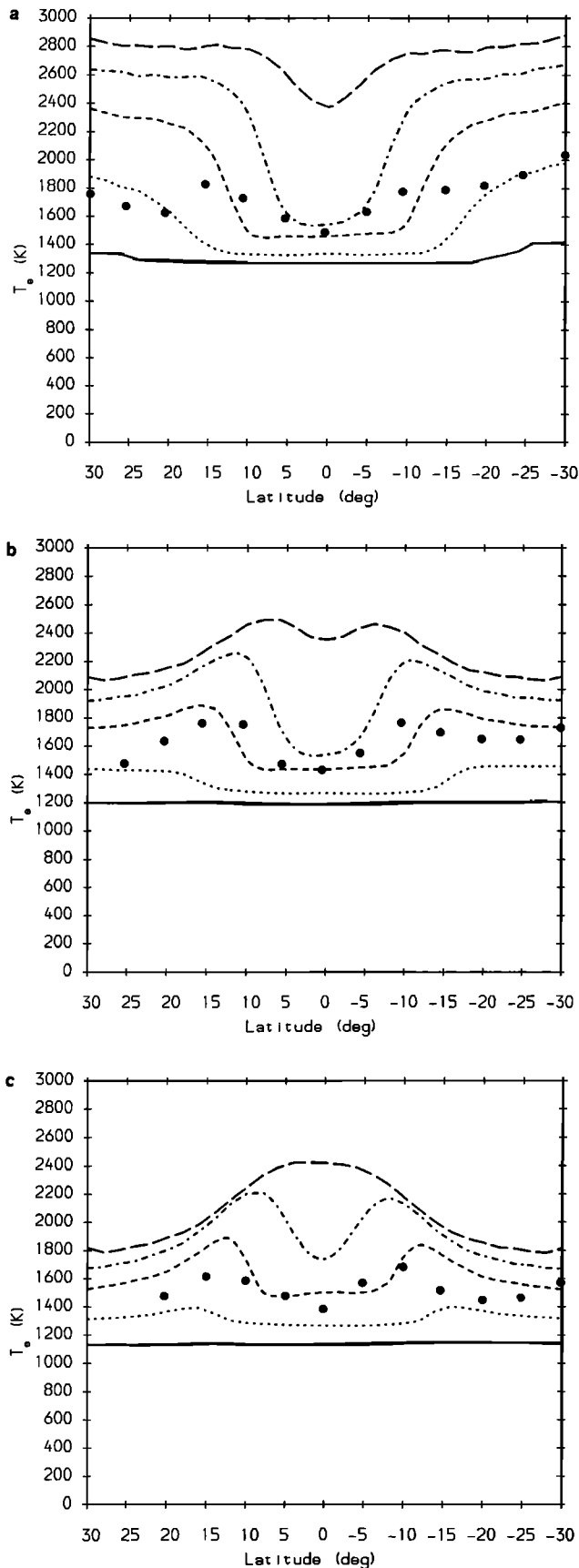
the conjugate ionosphere before being thermalized [Mantas *et al.*, 1978]. In the photoelectron heating code, backscattering is included self-consistently and pitch angle diffusion is taken care of by assuming that a fraction of the photoelectrons is trapped and that all the energy of the trapped flux is deposited in the plasmasphere. However, photoelectron trapping is not used in the present study as the study is for nighttime conditions.

Figures 6a, 6b, and 6c show the latitudinal variations of the model T_e at 1900 LT, 2000 LT, and 2100 LT, respectively. At each local time the variations are shown for five different altitudes (500, 650, 800, 950, 1100 km). At 1900 LT (Figure 6a) the latitudinal variation of T_e shows a minimum around the equator. This minimum, which depends on altitude, is caused mainly by the strong prereversal upward $E \times B$ drift which raises comparatively cold plasma from the bottomside ionosphere to the topside ionosphere in the form of a forward plasma fountain [Balan and Bailey, 1995]. At 2000 LT (Figure 6b), the variation of T_e shows crests on either side of the equator at altitudes above 800 km. At later times, as seen in Figure 6c, the crests appear at lower altitudes and disappear at higher altitudes; note the appearance of small crests at 650 km and the disappearance of the crests at 1100 km at 2100 LT (Figure 6c). At each altitude the T_e crests are found to fall on the same magnetic line of force, and they are found to occur slightly poleward of the ionization crests. The T_e crests arise from the combined effects of the evening prereversal upward $E \times B$ drift, postreversal downward $E \times B$ drift, and nighttime cooling. The downward $E \times B$ drift, which brings hot plasma from high altitudes and latitudes in the form of a reverse plasma fountain [Balan and Bailey, 1995; Balan *et al.*, 1996], causes the electron temperature to increase in the region of the plasma fountain. Outside this region, electron temperature decreases due to nighttime cooling. Consequently, T_e crests occur on either side of the equator before the equatorial T_e minimum (Figure 6a) disappears. The model values of ion temperatures (not shown) are found to be very nearly equal to the electron temperature; the ion temperatures are also found to exhibit the features shown in Figures 6a–6c.

3.2. Comparison Between Theory and Observation

In Figures 6a, 6b, and 6c the mean T_e values which were measured by Hinotori satellite in the time periods 1830–1930 LT, 1930–2030 LT, and 2030–2130 LT for $F_{10.7} > 250$ are also plotted as representative values at 1900 LT, 2000 LT, and 2100 LT, respectively. At 1900 LT, T_e shows a dip at around the equator and at 2000 LT and 2100 LT, T_e peaks appear at around ± 15 geomagnetic latitude. A comparison of the observations and model results at 2100 LT shows that the model T_e peak at 650 km is located about 2° – 3° poleward of the observed peaks. The magnitude of the model peak T_e almost agrees with the observation. Although the model does not fully reproduce the observations, the phenomenon can be explained as resulting from the plasma flows and plasma cooling during the evening hours.

The flows of plasma during evening hours as given by the model have been presented and explained by Balan and Bailey [1995] and Balan *et al.* [1996]. The plasma flows at 1900 LT and 2100 LT are shown in Figures 7a and 7b, respectively. During the prereversal period, the upward $E \times B$ drift raises comparatively cold plasma from the bottomside ionosphere to the topside ionosphere (Figure 7a); this causes low T_e around the equator as shown in Figure 6a. After the drift reverses from upward to downward, plasma from higher altitudes and lati-



tudes flows to lower altitudes and latitudes in the form of a reverse plasma fountain (Figure 7b). Near the equator (about $\pm 10^\circ$ in latitude) the temperature is still low because most of the uplifted cold plasma drifts down, while at around 10° – 20° in latitude most of the plasma flows down from higher altitude and therefore T_e is higher than near the equator. At latitudes outside the reach of hot plasma, where plasma is transported horizontally from higher latitudes but is still at lower altitudes than at latitudes 10° – 20° , the electron temperature is low and decreases due to nighttime cooling. Accordingly, the T_e observed by a satellite which crosses the magnetic field lines with high T_e shows two peaks, one in the north hemisphere and the other in south hemisphere (see Figure 1).

4. Discussion

The morphology of the EETA discussed in section 2 seems to be well explained on the basis of the plasma transport pattern in the evening equatorial ionosphere [Balan and Bailey, 1995]. It is clearly shown that the location of the T_e peaks coincide with the latitudinal position of the EIA crests, particularly in the equinoctial months of March–April and September–October (Figure 4). The thermospheric zonal wind (blowing away from the subsolar point) is generally strongest in the evening hours of these months [Hedin *et al.*, 1991]. This situation is conducive to the large amplitudes of the evening (pre-reversal) zonal electric field (vertical drift) enhancement [Batista *et al.*, 1986; Farley *et al.*, 1986] as well as of the vertical electric field (zonal plasma drift), thus contributing to the mechanism for the enhanced electron temperature as discussed in section 3. It is also interesting to note that the solar $F_{10.7\text{ cm}}$ flux controls both the vertical and zonal equatorial plasma drifts in the evening hours as discussed by Fejer *et al.* [1991]. For example, an increase of solar flux from 100 to 200 units could result in 100% increase in the yearly averaged vertical drift and by as much as 50% in the zonal plasma drift velocity. Therefore a large increase in the 10.7-cm solar flux should produce, as is evident from the EETA mechanism described above, hot plasma in the ionization anomaly region. The events centered around days 320, 340, and 400, that do not fall in the equinoctial months, are good examples of this effect. The factors which might be considered to explain the quantitative difference between the theory and observation, especially in height, might be the background density and the altitude variation of the upward plasma drift velocity. Another factor which might be taken into account is the neutral temperature. Raghvarao *et al.* [1991] reported that an eastward neutral wind is decelerated by ion-neutral drag and the bulk motion of the wind is converted to the kinetic temperature of neutral gases of about 50° . Accordingly, the energy loss rate of thermal electrons to the neutral gas is reduced which causes T_e to be higher than those without an enhancement in neutral gas temperature. Also, Sridharan *et al.* [1991] have found a high

Figure 6. (opposite) Theoretical model values of T_e plotted against geomagnetic latitude at five different altitudes (solid curve, 500 km; dotted curve, 650 km; short dashed curve, 800 km; dash-dotted curve, 950 km; and long dashed curve, 1100 km) for (a) 1900 LT, (b) 2000 LT, and (c) 2100 LT. Solid circles show mean T_e values observed by Hinotori for $F_{10.7} > 250$ during the time periods of 1830–1930 LT, 1930–2030 LT, and 2030–2130 LT.

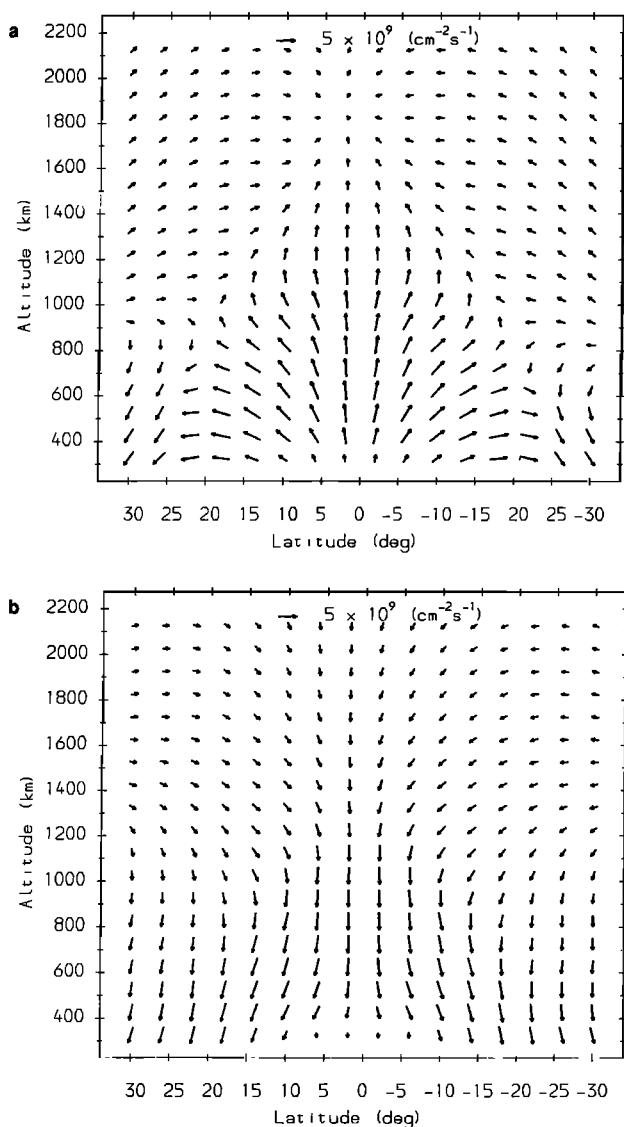


Figure 7. (a) Vector plasma fluxes at 1900 LT calculated under the same condition as for Figure 6. The fluxes are given in \log_{10} scale. The minimum vector length (zero length) corresponds to plasma flux less than $1 \times 10^8 \text{ cm}^{-2} \text{ s}^{-1}$. Positive latitude is northward. (b) Same as Figure 7a but at 2100 LT.

neutral temperature peak at 2100 LT in Indian longitude region. As yet, a reason for its occurrence has not been established.

5. Conclusions

The high electron temperature in the night time equatorial ionosphere discovered by the Japanese satellite Kyokko in 1978 was confirmed by the Hinotori satellite launched in 1981. A detailed study on the morphological features of the hot plasma region demonstrates that these regions are closely associated with the well known equatorial ionization anomaly during the postsunset hours. The hot plasma regions occur predominantly in the equinoctial months and show significant dependence on the intensity of solar 10.7 cm radio flux. The presently used theoretical ionosphere-plasmasphere models can predict the EETA, qualitatively. However, to understand

quantitatively, simultaneous measurements of the electron and ion temperatures and densities, vertical and horizontal plasma drifts, polarization electric field, neutral wind and ion composition in the 400–1000 km altitudes are needed. Such measurements could be accomplished by a multiple tethered satellite mission for which feasibility studies are being carried out.

Acknowledgments. We would like to express our sincere thanks to the satellite launching staff of ISAS and the related institutions. We are also grateful to late W. B. Hanson for his continuous encouragement. M. A. Abdu wishes to express his thanks to the Sao Paulo State Foundation for promotion of research (FAPESP) for the support received towards INPE-ISAS collaborations. N. Balan expresses his gratitude to ISAS for the award of a fellowship.

The Editor would like to thank K. Schlegel and T. Tanaka for their assistance in evaluating this paper.

References

- Abdu, M. A., I. S. Batista, G. O. Walker, J. H. A. Sobral, N. B. Trivedi, and E. R. de Paula, Equatorial ionospheric electric field during magnetospheric disturbances: Local time/longitude dependence from recent EITS campaigns, *J. Atmos. Terr. Phys.*, **57**, 1065–1083, 1995.
- Anderson, D. N., Modeling the ambient, low latitude F region ionosphere—A review, *J. Atmos. Terr. Phys.*, **43**, 753–762, 1981.
- Bailey, G. J., and N. Balan, A low-latitude ionosphere-plasmasphere model, in *STEP Hand Book*, edited by R. W. Schunk, p. 173, Utah State Univ., Logan, 1996.
- Bailey, G. J., R. Sellek, and Y. Rippeth, A modelling study of the equatorial topside ionosphere, *Ann. Geophys.*, **11**, 263–272, 1993.
- Bailey, G. J., N. Balan, and Y. Z. Su, The Sheffield University plasmasphere-ionosphere model—A review, *J. Atmos. Terr. Phys.*, in press, 1996.
- Balan, N., and G. J. Bailey, Equatorial plasma fountain and its effects: Possibility of an additional layer, *J. Geophys. Res.*, **100**, 21421–21432, 1995.
- Balan, N., G. J. Bailey, M. A. Abdu, K. I. Oyama, P. G. Richards, J. MacDougall, and I. S. Batista, Equatorial plasma fountain and its effects over three locations: Evidence for an additional layer, the F₃ layer, *J. Geophys. Res.*, in press, 1996.
- Banks, P. M., and A. F. Nagy, Concerning the influence of elastic scattering upon photoelectron transport and escape, *J. Geophys. Res.*, **75**, 1902–1910, 1970.
- Batista, I. S., M. A. Abdu, and J. A. Bittencourt, Equatorial F-region vertical plasma drift: Seasonal and longitudinal asymmetries in the American sector, *J. Geophys. Res.*, **91**, 12055–12064, 1986.
- Bilitza, D., International reference ionosphere 1990, URSI-COSPAR, Rep. NSSDC/WDC-A-R&S, 90-22, Natl. Space Sci. Data Cent., Lanham, Md., 1990.
- Farley, D. T., E. Bonelli, B. G. Fejer, and M. F. Larsen, The prereversal enhancement of the zonal electric field in the equatorial ionosphere, *J. Geophys. Res.*, **91**, 13723–13728, 1986.
- Fejer, B. G., E. R. de Paula, S. A. Ganguly, and R. F. Woodman, Average vertical and zonal plasma drifts over Jicamarca, *J. Geophys. Res.*, **96**, 13901–13906, 1991.
- Hanson, W. B., and R. J. Moffet, Ionization transport in the equatorial F region, *J. Geophys. Res.*, **71**, 5559–5572, 1966.
- Hedin, A. E., MSIS-86 thermospheric model, *J. Geophys. Res.*, **92**, 4649–4662, 1987.
- Hedin, A. E., et al., Revised global model of thermospheric winds using satellite and ground-based observations, *J. Geophys. Res.*, **96**, 7657–7688, 1991.
- Heelis, R. A., P. C. Kendall, R. J. Moffet, D. W. Windle, and H. Rishbeth, Electrical coupling of the E- and F-regions and its effects on F-region drifts and winds, *Planet. Space Sci.*, **22**, 743–756, 1974.
- Mantas, G. P., H. C. Carlson, and V. B. Wickwar, Photoelectron flux buildup in the plasmasphere, *J. Geophys. Res.*, **83**, 1–15, 1978.
- Moffet, R. J., The equatorial anomaly in the electron distribution of the terrestrial F-region, *Fundam. Cosmic Phys.*, **4**, 313–391, 1979.
- Oyama, K.-I., and K. Schlegel, Anomalous electron temperature above the South American Magnetic Anomaly, *Planet. Space Sci.*, **32**, 1513–1522, 1984.

- Raghavarao, R., L. E. Wharton, N. W. Spencer, H. G. Mayr, and L. H. Brace, An equatorial temperature and wind anomaly (ETWA), *Geophys. Res. Lett.*, *18*, 1193–1196, 1991.
- Richards, P. G., and D. G. Torr, Ratios of photoelectron to EUV ionization rates for aeronomic studies, *J. Geophys. Res.*, *93*, 4060–4066, 1988.
- Rishbeth, H., Polarization fields produced by winds in the equatorial *F* region, *Planet. Space Sci.*, *19*, 357–367, 1971.
- Sridharan, R., S. Gurubaron, R. Raghavarao, and R. Suhasini, Coordinated thermospheric and *F* region measurements from low latitudes, *J. Atmos. Terr. Phys.*, *53*, 515–519, 1991.
- Tobiska, W. K., Revised solar extreme ultraviolet flux model, *J. Atmos. Terr. Phys.*, *53*, 1005–1017, 1991.
- Torr, M. R., D. G. Torr, P. G. Richards, and S. P. Yung, Mid- and low-latitude model of thermospheric emissions, 1, $O^+(2P)$ 7320 Å and $N_2(2P)$ 3371 Å, *J. Geophys. Res.*, *95*, 21147–21168, 1990.
- Walker, G. O., and H. F. Chan, Computer simulation of seasonal variation of the ionospheric equatorial anomaly in East Asia under solar minimum condition, *J. Atmos. Terr. Phys.*, *51*, 953–974, 1989.
- Woodman, R. F., Vertical drift velocities and east-west electric fields at the magnetic equator, *J. Geophys. Res.*, *75*, 6249–6259, 1970.
- M. A. Abdu, I. S. Batista, and E. R. de Paula, National Institute for Space Research, INPE 12.225, Sao Jose dos Campos, Brazil.
- G. J. Bailey, Applied Mathematics Section, School of Mathematics, University of Sheffield, Sheffield S3 7RH, England.
- N. Balan and K.-I. Oyama, Institute of Space and Astronautical Science, Yoshinodai, Sagamihara 229, Japan.
- F. Isoda, Faculty of Education, Yokohama National University, Hodogaya, Yokohama 240, Japan.
- H. Oya, T. Takahashi, and S. Watanabe, Faculty of Science, Tohoku University, Aoba, Sendai 980-77, Japan.

(Received December 27, 1995; revised June 7, 1996; accepted June 14, 1996.)